exhibit kinetics that are sensitive to the viscosity of the solvent. This behavior has been observed recently in ligand binding by heme proteins.[4,31] Formal methods for analyzing such gate/intrinsic decompositions are currently being developed (J. A. McCammon and S. H. Northrup); these methods are analogous to those presented recently for gated diffusion-influenced reactions.[32-34]

The important result that transient packing defects and gating play essential roles in local conformational changes within proteins illustrates that the protein matrix exhibits both liquid-like and solid-like characteristics.[2] The initial displacements of groups are facilitated by small packing defects similar to those that facilitate atomic diffusion in simple liquids.[14] Proteins differ from simple liquids, however, in that their extensive covalent and hydrogen bonding limits the compliance of the matrix to larger deformations. Thus, the matrix displays elastic behavior analogous to that of a solid in response to large displacements of groups.[2]

Finally, it should be noted that the methods employed in this study will be useful in the analysis of other group displacements in proteins. The construction of a suitable reaction coordinate is an essential first step in the theoretical calculation of rate constants, activation parameters, and other characteristics of reactions in proteins.[20] The present results make clear that it is necessary to include gating effects explicity in the construction of reaction coordinates for processes that involve substantial group displacements. In the ring rotational isomerization case, the virtual dihedral angle χ_v serves as a probe of the gate configuration. It is also clear that Voronoi polyhedra provide a valuable quantitative measure of the contribution of transient packing defects to group displacements in proteins.

Acknowledgment. We thank Drs. Bennett Fox and Witold Brostow for providing a copy of the Voronoi polyhedron program. This research was supported in part by grants from the Robert A. Welch Foundation and the NSF (Houston) and from the Petroleum Research Fund as administered by the American Chemical Society, and the Research Corp. (TN). C.Y.L. was a Welch Foundation Postdoctoral Fellow. J.A.M. is an Alfred P. Sloan Fellow and recipient of an NIH Research Career Development Award.

Registry No. BPTI, 9087-70-1; L-tyrosine, 60-18-4.

(31) Beece, D.; Eisenstein, L.; Frauenfelder, H.; Good, D.; Marden, M. C.; Reinisch, L.; Reynolds, A. H.; Sorensen, L. B.; Yue, K. T. *Biochemistry* **1980**, *19*, 5147.
(32) McCammon, J. A.; Northrup, S. H. *Nature (London)* **1981**, *293*, 316.
(33) Northrup, S. H.; Zarrin, F.; McCammon, J. A. *J. Phys. Chem.* **1982**, *86*, 2314.
(34) Szabo, A.; Shoup, D.; Northrup, S. H.; McCammon, J. A. *J. Chem. Phys.* **1982**, *77*, 4484.

Conformational Analysis of Proline Rings from Proton Spin–Spin Coupling Constants and Force-Field Calculations: Application to Three Cyclic Tripeptides[1a,b]

Frank A. A. M. de Leeuw,[1c] Cornelis Altona,*[1c] Horst Kessler,[1d] Wolfgang Bermel,[1d] Axel Friedrich,[1d] Gerhard Krack,[1d] and William E. Hull[1e]

Contribution from the Gorlaeus Laboratories, University of Leiden, 2300 RA Leiden, The Netherlands, Institut für Organische Chemie der Universität Frankfurt, Niederurseler Hang, D-6000 Frankfurt-50, Federal Republic of Germany, and Bruker Analytische Messtechnik GmbH, Silberstreifen, D-7512, Rheinstetten-Fo, Federal Republic of Germany (FRG). *Received July 21, 1982*

Abstract: The conformational analysis of the proline rings in the cyclic tripeptides *cyclo*(L-Pro$_3$), *cyclo*(L-Pro$_2$-D-Pro), and *cyclo*(L-Pro-BzlGly-D-Pro) is carried out by means of the vicinal proton spin–spin coupling constants. The combined use of a generalized Karplus equation and the concept of pseudorotation afforded a detailed description of the conformational behavior of each Pro ring in solution. The results correlate well with the spin–lattice ^{13}C relaxation time data obtained previously and with force-field calculations carried out on the three molecules. Experimental differences between pairs of cis couplings are explained in terms of contributions of alternative coupling pathways. Comparison with the geometries obtained by means of crystallographic analysis shows that in each case the conformation of the prolyl residues in the tripeptides found in the solid state also predominates in solution: in *cyclo*(L-Pro$_3$) between ${}^{\beta}_{\alpha}T$(C$^{\beta}$exo-C$^{\alpha}$endo) and ${}^{\beta}$E; in *cyclo*(L-Pro^1-L-Pro^2-D-Pro^3), first residue ${}^{\gamma}E$, second residue ${}^{\gamma}_{\beta}T$, and D-Pro^3 ${}^{\beta}E$; in *cyclo*(L-Pro^1-BzlGly-D-Pro^3), first residue ${}^{\gamma}_{\beta}T$, third residue ${}^{\beta}E$ (T and E are the twist and evelope conformation in the usual convention). According to the ^1H NMR analysis and force-field calculation *cyclo*(L-Pro$_3$) appears to adopt a conformationally pure crown conformation in solution. The three Pro residues oscillate over an unusually large range within a (quasi) double-minimum energy well. The backbone of *cyclo*(L-Pro^1-L-Pro^2-D-Pro^3) adopts a twist-boat conformation, which allows L-Pro^1 and L-Pro^2 sufficient conformational freedom to flip over into a (minor) ${}_{\gamma}E$ form. D-Pro^3 again oscillates over a large range. The situation is more complicated in the case of the third cyclic tripeptide *cyclo*(L-Pro^1-BzlGly-D-Pro^3). Force-field calculations suggest the existence of two twist-boat conformers, *TB*-1 and *TB*-2, which interconvert via a boat form with $\phi_2 \sim 0°$. Since it is also predicted that the Pro residues in each of these *TB*'s enjoy some conformational freedom, a multistate mixture is envisaged.

The conformational analysis of the proline ring is discussed in a large number of papers; cf. ref 2-7. In contrast to the fairly rigid chair form of six-membered rings, five-membered rings in general demonstrate pseudorotational mobility. The conforma-

(1) (a) Peptide Conformations. 20. Previous paper in this series: Kessler, H. *Angew. Chem.* **1982**, *94*, 509-520. (b) Related previous paper: Kessler, H.; Bermel, W.; Friedrich, A.; Krack, G.; Hull, W. E. *J. Am. Chem. Soc.* **1982**, *104*, 6297-6304. (c) University of Leiden. (d) University of Frankfurt. (e) Bruker Analytische Messtechnik.

(2) Kessler, H.; Friedrich, A.; Hull, W. E. *J. Org. Chem.* **1981**, *46*, 3892-3895.
(3) (a) Deber, C. M.; Torchia, D. A.; Blout, E. R. *J. Am. Chem. Soc.* **1971**, *93*, 4893-4897. (b) Anteunis, M. J.; Callens, R.; Asher, V.; Sleeckx, J. *Bull. Soc. Chim. Belg.* **1978**, *87*, 41-60.

0002-7863/83/1505-2237$01.50/0

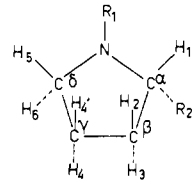

Figure 1. Labeling of carbon atoms and protons in L-proline. In D-proline the labeling is according to the mirror image.

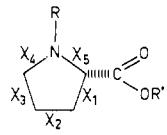

Figure 2. Conventional χ notation of endocyclic torsion angles in proline.

Table I. Correspondence between the Phase Angle P (deg) in Prolines and the Symmetrical Envelope (E) and Twist (T) Conformations

P_N	−72	−54	−36	−18	0	18	36	54	72
	${}^{\alpha}_{N}T$	${}^{\alpha}E$	${}^{\alpha}_{\beta}T$	${}_{\beta}E$	${}^{\beta}_{\gamma}T$	${}^{\gamma}E$	${}^{\gamma}_{\delta}T$	${}_{\delta}E$	${}^{N}_{\delta}T$
P_S	108	126	144	162	180	198	216	234	252
	${}^{N}_{\alpha}T$	${}_{\alpha}E$	${}^{\beta}_{\alpha}T$	${}^{\beta}E$	${}^{\beta}_{\gamma}T$	${}_{\gamma}E$	${}^{\delta}_{\gamma}T$	${}^{\delta}E$	${}^{\delta}_{N}T$

tional behavior of a given proline ring therefore will be dependent on its environment: thus not only the primary structure of the peptide, but also crystal packing forces and perhaps solvent effects are expected to influence the ring conformations and geometries to some extent. Nevertheless, the proline ring in open-chain peptides tends to have outspoken conformational preferences and appears less "floppy" than often thought.

A decade ago, Balasubramian et al.[5] proposed, from a statistical analysis of the then available crystal structures of prolyl residues, that the proline ring system prefers either of two conformations in the solid state: both visualized as "envelope" forms (${}^{\gamma}E$ and ${}_{\gamma}E$, also called A and B, respectively) with the atoms C^{δ}–N–C^{α}–C^{β} (see Figure 1) nearly coplanar and C^{γ} either above (${}^{\gamma}E$) or below (${}_{\gamma}E$) this plane. In the ${}_{\gamma}E$ form (C^{γ}-exo) the α-C'OR group in L-Pro points downward. With a growing number of crystal structures and analysis of the endocyclic torsion angles in terms of pseudorotation equation,[8] it became clear[6,7] that in the solid state the geometries are not restricted to the ${}^{\gamma}E$ and ${}_{\gamma}E$ conformations. Each of the classical A and B structures[5] actually represents a certain range of accessible conformations encompassing several E (envelope) and T (twist) forms.

The conformational behavior of the proline ring in solution can be deduced from the vicinal proton–proton NMR coupling constants. ${}^{3}J_{HH}$ depends strongly: (i) on the torsion angle between the two coupling protons,[9] (ii) on the electronegativity of substituents,[10] and (iii) on the orientation of the electronegative substituents.[11] In the past a number of functions which serve to describe the relation between ${}^{3}J_{HH}$ and ϕ_{HH} in amino acids have been proposed.[3a,12-14] Several workers (cf. ref 3a, 4, 15) have

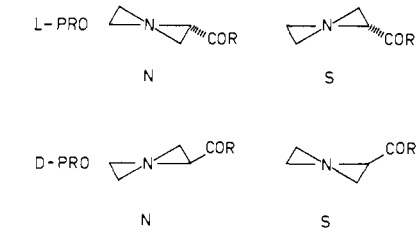

Figure 3. Perspective drawing of the N- and S-type conformations in L-proline (top) and D-proline (bottom).

attempted to calculate individual values for χ_1, χ_2, and χ_3 (see Figure 2) from coupling constants along the corresponding bonds. In so doing one ignores the fact that the endocyclic torsion angles in a five-membered ring are interrelated via the pseudorotation eq 1,[8] where P represents the phase angle of pseudorotation and

$$\chi_j = \chi_m \cos(P + ((j-2)4\pi)/5) \qquad j = 1 \ldots 5 \qquad (1)$$

χ_m is the puckering amplitude, i.e., the maximum value of χ_j attainable upon pseudorotation. With the aid of the concept of pseudorotation, it is possible to give an unambiguous description of a given proline geometry in terms of two parameters: P and χ_m. The correspondence between P and the usual envelope (E) and twist (T) conformational notation is shown in Table I, but note that the actual conformation usually does not occur at even or odd multiples of 18°; i.e., the actual conformation is not a priori a pure envelope or twist form, but somewhere "in between". Now the conformations of the L-proline ring can be separated into two broad classes depending on the sign of χ_2: a positive (according to the Klyne–Prelog[16] convention) χ_2 value defines the N-type proline conformations ($-90° \leq P \leq 90°$; a negative value of χ_2 defines the S-type proline conformations ($90° < P < 270°$) (see Figure 3). This classification in N- and S-type conformers[7] widens the original definition of C^{γ}-exo (${}^{\gamma}E$, P 18°) and C^{γ}-endo (${}_{\gamma}E$, P 162°) forms and encompasses families of related geometries. In D-proline rings the configuration around the C^{α} atom is reversed. If one sticks to the definition of "endo" and "exo" with respect to the α-C'OR group, this implies that in D-proline the N and S forms are mirror images of the N and S forms of L-proline (see Figure 3). Therefore, by definition the N family of forms in the D series is characterized by a negative value of χ_2. In practice one adds 180° to the phase angle calculated by eq 1. Now a direct comparison between P values of L and D residues can be made: a conformation described by given P and χ_m values will have equal coupling constants and, in absence of more chiral centers, equal energy in both D and L series.

The transition points between the N and S conformational ranges (χ_2 0°) are defined by ${}^{N}E$, P 90° and ${}_{N}E$, P 270°. According to reported force-field calculations[6] the regions about these points represent energy barriers that separate low-energy conformational ranges in pseudorotation space. The planar proline ring is estimated to lie about 3 kcal/mol above the global minima[6] located near to the centers of the N and S regions, P 0° and P 180°, respectively. The calculated saddle point[6] (2.7 kcal/mol) of the transition between the N- and S-type conformers occurs near P 90° and corresponds to a severely flattened proline ring.

In previous papers of the Leiden group[17,18] a new empirical generalization of the Karplus equation[9] was introduced. This six-parameter equation explicitly takes into account the effect of orientation of electronegative substituents with respect to the coupling vicinal protons. The parametrization was carried out on a large set of experimental data derived from well-defined six-membered rings, but subsequent work showed that these parameters could be used with confidence for the description of the five-membered ribose rings in nucleic acids[19,20] and of prolines.[7]

(4) Bach, A. C.; Bothner-By, A. A.; Gierasch, L. M. *J. Am. Chem. Soc.* **1982**, *104*, 572–576.
(5) Balasubramanian, R.; Lakshminarayanan, A. V.; Sabesan, M. N.; Tegoni, G.; Venkatesan, K.; Ramachandran, G. N. *Int. J. Pept. Protein Res.* **1971**, *3*, 25–33.
(6) DeTar, D. F.; Luthra, N. P. *J. Am. Chem. Soc.* **1977**, *99*, 1232–1244.
(7) Haasnoot, C. A. G.; De Leeuw, F. A. A. M.; De Leeuw, H. P. M.; Altona, C. *Biopolymers* **1981**, *20*, 1211–1245.
(8) Altona, C.; Geise, H. J.; Romers, C. *Tetrahedron* **1968**, *24*, 13–32. Altona, C.; Sundaralingam, M. *J. Am. Chem. Soc.* **1972**, *94*, 8205–8212.
(9) Karplus, M. *J. Chem. Phys.* **1959**, *30*, 11–15.
(10) Glick, R. E.; Bothner-By, A. A. *J. Chem. Phys.* **1965**, *25*, 362–363.
(11) Abraham, R. J.; Gatti, G. *J. Chem. Soc. B* **1969**, *961*–968. Pachler, K. G. R. *Tetrahedron Lett.* **1970**, 1955–1958; *Tetrahedron* **1971**, *27*, 187–199.
(12) Pachler, K. G. R. *Spectrochim. Acta* **1964**, *20*, 581–587.
(13) Pogliani, L.; Ellenberger, M.; Valet, J.; Bellocq, A. M. *Int. J. Pept. Protein Res.* **1975**, *7*, 345–360 and references cited therein.
(14) Bystrov, V. F. *Progr. Nucl. Magn. Reson. Spectrosc.* **1976**, *10*, 41–81 and references cited therein.
(15) Abraham, R. J.; Thomas, W. A. *J. Chem. Soc.* **1964**, *3739*–3748.
(16) Klyne, W.; Prelog, V. *Experimentia* **1960**, *16*, 521–523.
(17) Haasnoot, C. A. G.; de Leeuw, F. A. A. M.; Altona, C. *Tetrahedron* **1980**, *36*, 2783–2792.
(18) Haasnoot, C. A. G.; de Leeuw, F. A. A. M.; Altona, C. *Bull. Soc. Chim. Belg.* **1980**, *89*, 125–131.

The concept of pseudorotation combined with the generalized Karplus equation[17] offers the possibility to deduce the solution geometry from the information afforded by all 10 coupling constants of a proline ring simultaneously. This objective was realized by the computer program PSEUROT[21] which utilizes an iterative least-squares procedure.

In the preceding paper of the Frankfurt group[1b] the ^{1}H NMR analysis of *cyclo*(L-Pro-L-Pro-D-Pro), abbreviated (L-L-D), by means of two-dimensional spectroscopic techniques was reported. This analysis provided reliable coupling constant data on three different prolyl residues in a single molecule which, moreover, has been investigated by other techniques such as X-ray analysis[22,23] and ^{13}C NMR spectroscopy in solution[24,25] and in the solid state.[26] The coupling constants of *cyclo*(L-Pro$_3$), abbreviated (L_3), which molecule has an effective C_3 symmetry in solution and could be analyzed as a seven-spin system, is described in an earlier report.[2] In addition, the 500-MHz ^{1}H NMR analysis of a third cyclic tripeptide, *cyclo*(L-Pro-BzlGly-D-Pro), abbreviated (L-0-D), is now available.[27]

In the present paper we present the detailed pseudorotational analysis of the prolyl residues in these molecules, based on experimental coupling constants, with three objectives in mind: (i) the determination of the N/S equilibrium constant in solution, (ii) the determination of the geometry of the major species, N or S, in terms of phase angle P_N and P_S and puckering amplitude χ_N and χ_S, and (iii) the determination of the conformational behavior of the nine-membered ring in cyclotripeptides.

It is important to remember that changes in a given backbone angle ϕ(C′–N–C$^\alpha$–C′) will affect the corresponding endocyclic torsion angle χ_5 and thus the conformational preferences of the attached proline ring. In other words, an equilibrium between, say, two different forms of the nine-atom cycle can be reflected by the conformational behavior of the prolyl residues, i.e., points (i) and (ii) above. Because of the fact that the backbone angles ψ(N–C$^\alpha$–C′–N) and ω(C$^\alpha$–C′–N–C) escape detection by ^{1}H NMR spectroscopy, it was considered worthwhile to take recourse to valence-force-field calculations in order to guide the interpretation of the experimental results. It will be shown that the major conformational features of these cyclotripeptides correspond to those deduced from X-ray crystallography but that in solution these molecules or parts thereof have access to hitherto undetected degrees of conformational freedom.

Procedure

The basic equations that are utilized in the computer program PSEUROT[21] are summarized as follows:

The torsion angles between C–H vectors, ϕ_{HH} and the corresponding endocyclic torsion angle χ_1, χ_2, and χ_3 are related via eq 2. In the usual

$$\phi_{HH} = \chi_m \cos (P + \text{phase}) + \text{angle} \quad (2)$$

approximation of trigonal projection symmetry the angle parameter is zero for cis couplings and ±120° for trans couplings. We prefer to take deviations from 120° symmetry into account. The actual parameters used have been published previously.[7]

The proline system under investigation can be engaged in a fast conformational equilibrium. The two-state model is described by

$$N \underset{}{\overset{K}{\rightleftharpoons}} S$$

In this case, the observed coupling constants represent a time-average value, eq 3, where X_N and X_S are mole fractions ($X_N + X_S = 1$) and J_N

$$J_{exp} = X_N J_N + X_S J_S \quad (3)$$

and J_S represent any of the 10 coupling constants in the pure conformers. In unsubstituted prolines the H–C–C–H fragments along the C$^\beta$–C$^\gamma$ and C$^\gamma$–C$^\delta$ bond carry two substituents and the generalized Karplus equation takes the form[17]

$$^3J_{HH} = 13.70 \cos^2 \phi_{HH} - 0.73 \cos \phi_{HH} + \sum \Delta E_i (0.56 - 2.47 \cos^2 (\xi_i \phi_{HH} + 16.9 |\Delta E_i|)) \quad (4)$$

in which ϕ_{HH} is the Klyne–Prelog[16] signed proton–proton torsion angle and ΔE_i denotes the differences in electronegativity between the substituent S_i and hydrogen on the Huggins' scale[28] corrected for the influence of β substituents;[17] ξ_i stands for +1 or −1 according to the orientation of the substituent S_i with respect to the coupling proton on the same carbon atom.[17] For the trisubstituted H–C–C–H fragment along the C$^\alpha$–C$^\beta$ bond, the same generalized Karplus equation is utilized with slightly modified empirical parameters,[17] eq 5.

$$^3J_{HH} = 13.22 \cos^2 \phi_{HH} - 0.99 \cos \phi_{HH} + \sum \Delta E_i (0.87 - 2.46 \cos^2 (\xi_i \phi_{HH} + 19.9 |\Delta E_i|)) \quad (5)$$

The complete PSEUROT analysis entails the least-squares optimization of five independent parameters, i.e., "best values" of P_N, χ_N, P_S, χ_S, and K, from 10 couplings. A good measure of the "quality" of the analysis and of the reliability of the model used is afforded by the rms (root mean square) deviation between observed and calculated coupling constants and by the absence of gross individual differences. Typical rms values for a large series of prolines[7] range from 0.25 to 0.5 Hz. In view of our earlier error estimation[17] this is considered satisfactory for a well-behaving two-state system. However, the Barfield transmission effect (vide infra) can cause the rms to increase by an estimated 0.1–0.2 Hz. Therefore, it is not easy to rigorously define the limit of acceptability. In our opinion, an rms ≥ 1 Hz indicates serious errors in the model used.

The program has a built-in option which allows one to constrain one (or more) of the five parameters to a preset value. This feature is especially important in cases where the conformational equilibrium is heavily biased toward one side and experimental errors in the coupling constants would tend to produce unrealistic pseudorotation parameters for the less abundant conformer. Moreover, a constraint of 1.0 on one of the mole fractions implies the assumption of a single-state model. When the rms value drops significantly when this constraint is lifted, this can be considered evidence against the applicability of the single-state approximation. Complications may arise, however. It will be shown below that in some instances the calculated two-state parameters do not appear to reflect physically separated conformers and a more refined approach is called for. Indeed, in these cases force-field calculations indicate the existence of a skewed potential energy well which allows the proline ring to carry out large-amplitude anharmonic oscillations. Details concerning the force-field calculations will be given in the appropriate section.

Results and Discussion

First, we report the pseudorotation analysis of the prolyl residues in the three cyclic tripeptides purely on the basis of the measured coupling constants. The pseudorotation parameters obtained for the various possible models and the resulting rms values are collected in Table II. A comparison between observed and a selection of calculated couplings is given in Table III. A translation of the pseudorotation parameters into individual endocyclic torsion angles χ_i is presented in Table IV. Tables II and IV also contain the corresponding data from X-ray crystallography and the results from our present force-field minimizations. Next, the spin–lattice relaxation data are discussed, followed by some remarks concerning alternative coupling pathways. Finally, the conformational preference of the cyclic peptide backbone and its effect on the behavior of the prolyl residues will be discussed in the light of the force-field calculations.

***cyclo*(L-Pro$_3$).** The pseudorotational analysis of the prolyl residues in (L_3) was started on the assumption of the existence of a single conformational species in solution; i.e., the mole fraction of S-type conformer was constrained to be 1.0 and P_S and χ_m were allowed to vary. This approach yielded an S conformer with P 139° but at the same time a rather high rms value, 1.10 Hz.

(19) Haasnoot, C. A. G.; de Leeuw, F. A. A. M.; de Leeuw, H. P. M.; Altona, C. *Org. Magn. Reson.* **1981**, *15*, 43–52.
(20) De Leeuw, F. A. A. M.; Altona, C. *J. Chem. Soc., Perkin Trans. 2* **1982**, 375–384.
(21) De Leeuw, F. A. A. M.; Altona, C. *J. Compt. Chem.*, in press.
(22) Bats, J. W.; Friedrich, A.; Fuess, H.; Kessler, H.; Mästle, W.; Rothe, M. *Angew. Chem.* **1979**, *91*, 573–574; *Angew. Chem., Int. Ed. Engl.* **1979**, *18*, 538–539.
(23) Bats,m, J. W.; Fuess, H. *J. Am. Chem. Soc.* **1980**, *102*, 2065–2070.
(24) Friedrich, A. Thesis, Frankfurt, 1980.
(25) Krack, G. Thesis, Frankfurt, 1981. Kessler, H.; Bermel, W.; Hull, W. E.; Krack, G., unpublished.
(26) Kessler, H.; Bermel, W.; Friedrich, A. *Angew. Chem.*, in press.
(27) Kessler, H.; Bermel, W.; Hull, W. E.; Krack, G.; Bats, J. W.; Fuess, H., submitted for publication.
(28) Huggins, M. L. *J. Am. Chem. Soc.* **1953**, *75*, 4123–4126.

Table II. Geometry and Distribution of Proline Conformations in *cyclo*(L-Pro$_3$), *cyclo*(L-Pro$_2$-D-Pro), and *cyclo*(L-Pro-BzlGly-D-Pro) Calculated from NMR Coupling Constants[a] (for Purposes of Comparison a Selection[b] of Pseudorotation Parameters Calculated from X-ray Data and from Force-Field (FF) Calculations Is Also Shown)

calcn no.	compd	method	model used	P_N	χ_N	P_S	χ_S	X_S[c]	rms, Hz
1	(L_3)	NMR	*d*			139	36	1.0*	1.07
2			*e*	91	42*	158	42*	0.65	0.61
3			*e*	75*	40*	152	40	0.75	0.64
4			*f*			139	42		0.66
		X-ray[g]				148	33		
		FF		75	32	155	35		
	(L^1-L^2-D^3)								
5	L^1	NMR	*d*	17	38			0.0*	1.53
6			*e*	16	44	162[j]	40*	0.21	0.49
		X-ray[h]		17	42				
		FF	*NNS/SNS*	11	35	191	32		
7	L^2	NMR	*d*	−2	32			0.0*	2.58
8			*e*	−7	47	209	40*	0.37	0.45
		X-ray[h]		−4	38				
		FF	*NNS/NSS*	−3	35	198	35		
9	D^3	NMR	*d*			153	41	1.0*	0.77
10			*e*	90*	40*	157	44	0.88	0.66
11			*e*	75*	40*	155	43	0.91	0.67
12			*f*			153	43		0.67
		X-ray[h]				146	39		
		FF	*NNS*			144	40		
	(L^1-0-D^3)								
13	L^1	NMR	*d*	5	30			0.0*	2.06
14			*e*	6	42	154	40	0.33	0.39
		X-ray[i]		10	37				
		FF	*TB*1	9	35	192	33		
			*TB*2			144	40		
15	D^3	NMR	*d*			156	40	1.0*	1.03
16			*e*	68	40*	160	45	0.82*	0.50
17			*f*			155	44		0.67
		X-ray[i]				160	40		
		FF	*TB*1			145	40		
			*TB*2	−6	35	201	34		

[a] Constrained parameters are marked with an asterisk. [b] All three compounds crystallize with two crystallographically independent molecules in the unit cell. In each case we have selected the Pro ring which has a geometry closest to the one calculated from the NMR data. This was done because these "soft" conformations appear easily deformable by crystal packing forces and the X-ray structure does not tell us which of the individual ring forms occur closest to the form adopted in solution. [c] Mole fraction of *S* conformer. [d] Single state model. [e] Two-state model. [f] Oscillating single-state model. [g] Reference 29. [h] Reference 23. [i] Reference 33. [j] In another calculation P_S was fixed at 190°. The rms value increased only slightly as a result, i.e., 0.53 Hz.

Table III. Sample Calculations of Coupling Constants (Hz) in *cyclo*(L-Pro$_3$),[a] *cyclo*(L-Pro$_2$-D-Pro),[b] and *cyclo*(L-Pro-BzlGly-D-Pro)[c] (Calculation Numbers Correspond to Those Shown in Table II)

calcn no.	compd		1-2	1-3	2-4	3-4	2-4′	3-4′	4-5	4-6	4′-5	4′-6
	(L-L-L)											
		exptl	7.31	0.69	10.03	8.55	9.66	2.44	6.92	10.22	9.16	4.66
3		calcd	7.35	1.54	9.33	8.73	8.90	1.79	6.24	9.57	9.46	3.72
	(L^1-L^2-D^3)											
	L^1	exptl	7.07	7.59	3.40	7.09	7.00	10.78	3.07	6.69	7.78	9.89
6		calcd	7.36	7.92	2.96	6.85	6.69	9.92	2.38	6.84	7.14	9.41
	L^2	exptl	6.99	8.22	4.90	7.15	5.92	8.29	4.90	8.04	6.88	7.61
8		calcd	6.85	8.12	4.74	6.60	6.52	8.32	4.54	7.16	7.27	7.09
	D^3	exptl	6.51	0.58	11.94	7.31	8.29	1.25	8.98	10.23	9.11	3.30
11		calcd	6.59	1.28	11.30	7.45	7.69	0.90	8.06	9.55	9.29	1.97
12		calcd	6.70	1.17	11.48	7.68	7.93	0.50	8.06	9.54	9.28	1.98
	(L^1-0-D^3)											
	L^1	exptl	6.88	6.95	4.69	7.08	7.20	9.39	3.28	8.33	8.33	8.21
14		calcd	6.81	7.32	4.17	7.07	6.98	8.50	3.02	7.97	8.18	7.98
	D^3	exptl	6.75	1.55	11.03	7.23	7.89	2.27	8.80	9.49	8.59	3.45
16		calcd	6.79	1.57	10.60	7.24	7.44	1.79	7.94	8.83	8.59	2.60
17		calcd	7.10	1.54	10.79	7.97	8.19	0.96	7.88	8.96	8.73	2.56

[a] Data taken from ref 2. [b] Data taken from ref 1. [c] Data taken from ref 27.

Further calculations were carried out under the assumption of a two-state *N*/*S* equilibrium. It was found that strong correlations occurred between the calculated puckering amplitudes; i.e., these parameters could not be determined independently from each other. Therefore, the amplitudes χ_N and χ_S were constrained to assume standard values.[7] Trial calculations indicated that the final pseudorotation angles obtained hardly vary with the actual choice of χ_N and χ_S.

The final rms value dropped to 0.61 Hz and this, on first sight, appeared to indicate the presence of 35% of a second (minor) species participating in a conformational blend. The calculated geometry of the major species, P_S 158°, corresponds to $^{\beta}E$ and shows similarity to the geometry adopted by four out of six independent residues found in the solid state,[29] P_S 141–148°, $^{\beta}_{\alpha}T$. The geometry calculated for the minor species appears rather surprising, however: $P \sim 90°$, ^{N}E. The difference between calculated *P* values of the major and minor species, about 70°,

(29) Druyan, M. E.; Coulter, C. L.; Walter, R.; Karatha, G.; Ambady, G. K. *J. Am. Chem. Soc.* **1976**, *98*, 5496–5502.

Table IV. Endo Cyclic Torsion Angles (deg) of Proline Rings in *cyclo*(L-Pro$_3$), *cyclo*(L-Pro$_2$-D-Pro), and *cyclo*(L-Pro-BzlGly-D-Pro) in Solution, in the Solid State and from Molecular Mechanics, Calculated from the Pseudorotational Parameters Given in Table II (Calculation Numbers Correspond with Those Shown in Table II)

			N-type conformer[a]					*S*-type conformer[a]				
calcn no.	compd	method	χ_1	χ_2	χ_3	χ_4	χ_5	χ_1	χ_2	χ_3	χ_4	χ_5
	(L-L-L)											
3		NMR	14	10	−31	40	−34	40	−36	18	7	−30
4		NMR[b]						34	−26	8	13	−29
		X-ray						31	−24	7	14	−28
		FF	11	8	−24	33	−27	33	−31	17	5	−24
	(L^1-L^2-D^3)											
6	L^1	NMR	−27	42	−41	24	2	38	−38	24	0	−23
		X-ray	−25	41	−39	24	1					
		FF	−24	35	−32	17	4	22	−32	29	−16	−4
8	L^2	NMR	−41	46	−34	9	20	17	−35	40	−29	8
		X-ray	−32	39	−29	10	14					
		FF	−30	35	−27	9	13	21	−33	32	−20	0
11	D^3	NMR	−14	−10	31	−40	34	−42	39	−21	−5	29
12		NMR[c]						−39	36	−18	−6	28
		X-ray						−38	32	−14	−11	31
		FF						−39	33	−13	−13	33
	(L^1-0-D^3)											
14	L^1	NMR	−31	42	−37	17	9	39	−36	19	6	−28
		X-ray	−26	37	−33	17	5					
		FF *TB*1	−25	35	−31	16	5	22	−32	30	−17	−3
		*TB*2						40	−33	13	13	−33
16	D^3	NMR	−10	−15	34	−40	31	−43	43	−26	−1	28
		X-ray						−38	38	−22	−1	25
		FF *TB*1						−39	33	−14	−12	32
		*TB*2	30	−35	26	−8	−14	−19	32	−32	22	−2

[a] See Figure 2 for the χ angle notation. [b] Apparent χ_m 34°, actual χ_m 42°. [c] Apparent χ_m 40°, actual χ_m 43°.

is suspiciously small. One can hardly assume the existence of a conformational energy barrier large enough to physically separate two species that occur as close together as 70° on the pseudorotational itinerary, particularly in view of the fact that the nine-atom backbone ring is forced to adopt a single, well-defined, crown form.[30] For these reasons the two-state model appears questionable in this particular instance. For reasons explained later, a second two-state calculation was carried out with the parameters of the "minor form" fixed at P_N 75°, χ_N 40°, Table II. This minimization yielded virtually the same rms value as before, 0.64 Hz, and only slightly shifted parameters for the major form: P_S 152°, χ_S 40°, mole fraction X_S 0.75. The coupling constants calculated for this conformational mixture are shown in Table III.

At this stage of our investigations it was realized that the results of the calculations—a high rms value from the single-state model and a significant drop in the two-state calculation—perhaps could be explained in a different way, i.e., by the assumption of a single, but unusually broad and shallow, pseudorotational energy well centered at about $P = 139°$. The existence of a shallow potential energy well implies the occurrence of large-amplitude oscillations of the phase angle on a short (10^{-12}–10^{-13} s) time scale. The term "pseudolibration" for this phenomenon has been coined,[31] but in the following we prefer to use the term "oscillating single-state model".

The unequal relative conformational populations, calculated from the two-state model above, seem to indicate that the postulated energy well could be steeper in the direction of increasing P than in the direction of decreasing P, i.e., somewhat skewed. If this were the case, a correct calculation of the coupling constants would involve the calculation of a Boltzmann distribution on the basis of several unknown energy parameters. For this reason we preferred to limit our explorations to a simple one-parameter harmonic potential energy function of the usual type, eq 6, where

$$E(P) = 0.5V_1[1 - \cos(P - P_0)] \quad (6)$$

P_0 is varied about the value found in the single-state analysis, P 139°. When a continuous Boltzmann distribution is assumed, eq 7 is valid for each vicinal coupling:[32] $J(P)$ in eq 7 represents the

$$\langle J_i \rangle = \frac{\int_0^{2\pi} J(P) \exp(-E(P)/RT)}{\int_0^{2\pi} \exp(-E(P)/RT)} \quad (7)$$

coupling constant as a function of the phase angle of pseudorotation at constant puckering amplitude χ_m.

Equations 6 and 7 were combined with the previous eq 2, 4, and 5 in a computer program to yield, for each chosen combination of P_0 and χ_m, the optimum value of the energy parameter V_1 by means of a Newton–Raphson least-squares procedure which finds the best fit between observed and calculated coupling constants. The integrals in eq 7 and the first derivative of V_1 were evaluated numerically.

Several trial calculations were carried out for different input values of the puckering amplitude and phase angle. The "best fit" was obtained for P_S 139°, χ_S 42°, and V_1 = 3.5 kcal/mol: the residual rms value amounted to 0.66 Hz. This result is fairly sensitive toward the input phase angle; when P_S was fixed at 129° the rms value increased to over 0.8 Hz.

From a mathematical point of view both approaches, the two-state and the oscillating single-state model, yield equivalent results and cannot be discriminated. It is well to stress at this point that the calculated value of the energy barrier V_1 should not be taken too literally in view of the necessarily crude assumptions embodied in the oscillating single-state model. However, some experimental support for the latter model can be distilled from the X-ray investigation.[29] The two molecules of (L_3) in the asymmetric unit in the crystal afford information on the geometry of six prolyl residues in different surroundings. These six residues all occur in the same general region of pseudorotation space, and it is of interest to note that their phase angles run from 124° to 148°; i.e., it seems as if small differences in intermolecular surroundings can push the relatively "soft" proline conformation about within a relatively wide valley. If the additional assumption is

(30) Kessler, H. In "Stereodynamics of Molecular Systems"; Sarma, R. H., Ed.; Pergamon Press: New York, **1979**, 187–196. Kessler, H. Krämer, P.; Krack, G. *Isr. J. Chem.* **1980**, *20*, 188–195.

(31) Altona, C.; Buys, H. R.; Havinga, E. *Recl. Trav. Chim. Pays-Bas* **1966**, *85*, 973–982.

(32) Schug, J. C.; McMahon, P. E.; Gutowski, H. S. *J. Chem. Phys.* **1960**, *33*, 843–850.

made that crystal packing forces act in a random fashion, the average of the six geometries found in the crystal can be taken as a reasonable approximation for the free (L_3) molecule with 3-fold symmetry. These deductions can be tested in a straightforward manner by comparison with the results of the present oscillating single-state model. At constant puckering amplitude χ_m, eq 8 is valid where $\langle\chi_i\rangle$ represents the time-average χ_i. The

$$\langle\chi_i\rangle = \frac{\int_0^{2\pi} \chi(P)\, \exp(-E(P)/RT)}{\int_0^{2\pi} \exp(-E(P)/RT)} \qquad (8)$$

results are shown in Table IV, calculation 4. It is seen that the agreement between the mean X-ray structure and the conformation in solution derived from the oscillating single-state model appears excellent. It is pointed out that this model also explains the relatively small puckering amplitude found in the crystal, averaged χ_m 32.8°, as compared to the larger value extracted from the spin–spin coupling constants, χ_m 42°. The lower value now appears to be hitherto unsuspected but obvious consequence of large-amplitude oscillations of the phase angles of the prolyl residues in the crystal. These oscillations are also clearly reflected in the thermal parameters U as found in the solid state, particularly large U's are seen for C^β, C^γ, and C^δ.[29]

The force-field calculations, discussed below, corroborate these conclusions and at the same time suggest that the true potential energy well is indeed skewed in shape. However, further calculations of coupling constants on the basis of a skewed oscillating single-state model were not attempted.

***cyclo*(L-Pro¹-L-Pro²-D-Pro³).** As was the case for (L_3) discussed above, the pseudorotational analysis of (L-L-D) was started on the assumption of a single state present in solution. This resulted in rather large rms deviations for the L-Pro¹ and L-Pro² residues (>1.5 Hz). Further calculations on the basis of a two-state equilibrium composition yielded residual rms values of less than 0.5 Hz in both cases. The results are collected in Tables II and III. In surprising contrast to the analysis of (L_3), two discrete conformational species appear to exist in equilibrium: for L-Pro¹ a major N form (ca. 79%) has $P \sim 16°$ ($^\gamma E$) and a minor S conformer, $P \sim 162°$ ($^\beta E$); for L-Pro² we find again a major N form (ca. 63%), $P \sim -7°$ ($^\gamma_\beta T$) and a minor S species, $P \sim 209°$ (between $_\gamma E$ and $^\delta_\gamma T$). In the crystal structure[23] of this cyclic tripeptide two crystallographically independent molecules occur in the asymmetric unit, molecules A and B. Only the major N forms of L-Pro¹ and L-Pro² occur in the solid state. From the published atomic coordinates we have calculated the P_N and χ_N values for both molecules. For reasons outlined in footnote b, Table II, the values closest to the geometry deduced from NMR spectroscopy are shown in Table II for the sake of comparison. It is satisfactory to note the quite close similarity between the conformations of L-Pro¹ and L-Pro² as they occur in the crystal and those deduced for the solution. For the minor S forms no such comparison with the solid-state data can be made, but the present analysis appears to indicate that the phase angle P_S of the L-Pro¹ residue is smaller than that of the L-Pro² unit. It should be kept in mind, however, that the precision of the geometry determination is inevitably less than that of the major conformation.

The assumption of a single conformation in solution resulted for the D-Pro³ residue in an S conformer, $P \sim 153°$ (between $^\beta_\alpha T$ and $^\beta E$) and a rms deviation of 0.77 Hz. The two-state calculation appeared to yield a strongly biased blend, a major S form ($P_S \sim$ 157°, 88%) and a minor conformer with a rather ill-defined geometry; i.e., P could be varied between 60 and 110° without much effect on the geometry or mole fraction of the major conformer nor on the rms value, 0.65–0.68 Hz. Typical results are shown in Table II, calculations 10 and 11.

In the crystal structure of (L-L-D)[23] the phase angles calculated for the D-Pro³ ring span a relatively large pseudorotational range: molecule A, P 117°; molecule B, P 146°. This fact, as well as the unsatisfactory results from the two-state model, suggests that D-Pro³, like the L-Pro rings in (L_3), exists in a single broad pseudorotational energy well. The evaluation of the coupling constants by means of the oscillating single-state model yielded an rms deviation of 0.67 Hz, P_0 153° and χ_X 43°, Table II, calculation 12. The calculated value of V_1 appeared strongly dependent on small changes in P_0 (eq 6) and in χ_m and probably has no real physical significance.

It is clear from the above that the information available from NMR coupling constants does not allow a clear distinction between the two models for D-Pro³: two-state and oscillating single-state, and the force-field calculations proved indispensable to settle the matter, vide infra. A comparison between the observed $^3J_{HH}$ values and the values calculated for the two models is presented in Table III.

***cyclo*(L-Pro¹-BzlGly-D-Pro³).** The analysis of the coupling constants of (L-O-D) was again carried out in the way described above. The single-state model applied to L-Pro¹, yielded an rms value of 2.06 Hz and was rejected at once. The two-state model gave satisfactory results: a major N form (ca. 67%), with $P_N \sim$ 6° ($^\gamma_\beta T$), occurs in equilibrium with a minor S conformer, $P_S \sim$ 154° (between $^\beta_\alpha T$ and $^\beta E$); the final rms is 0.39 Hz, see Table II and III. The geometry of the major form again shows surprising conformity with the crystal structure data;[33] P_N values of −8° and 10° are found for L-Pro¹ in the two crystallographically independent molecules I and II.

The single-state approach, applied to the coupling constants of the D-Pro³ residue, yielded a residual rms of 1.03 Hz and P_S ~ 156°. The two-state calculation gave, not unexpectedly, a biased blend: a major S conformer (P_S 160°, 82%) and an ill-defined minor conformer ($P_N \sim 68°$), rms 0.50 Hz, see Table II, calculation 16. The oscillating single-state model in this case did not yield a comparable rms value. On the contrary, the best-fit parametrization yielded $P_0 \sim 155°$, $\chi_m \sim 44°$ and a residual rms of 0.67 Hz, Table II, calculation 17. A comparison of observed and calculated couplings for both models is presented in Table III.

Apparently, neither of the models affords a satisfactory description of the true state of affairs for D-Pro³. It will be shown below that our force-field calculations indicate the existence of two interconverting twist-boat forms for the nine-cycle backbone of (L-O-D) as it was previously postulated from geometrical considerations,[30] whereas (L-L-D) can assume only one twist-boat form. The latter already provides for a "two-state" behavior of the prolyl residues and it follows that two different twist-boats in the case of (L-O-D) in principle could give rise to a four-state conformational equilibrium for each proline. In other words, the "individual" N and S states detected in the two-state model calculations may well represent time-averages of two discrete conformational substates present within each (N or S) range. If this were the case, the coupling constant approach cannot help us to clarify the situation unless future measurements are carried out at temperatures sufficiently low so as to freeze out the two twist-boats on the NMR time scale. The attempt to slow down the equilibrium of the six degenerated boats in *cyclo*(Sar_3) and *cyclo*($BzlGly_3$) at −90 °C in CD_2Cl_2 failed.[25] Therefore, prospects do not look bright, because the same FF calculations also predict a low barrier between the two twist-boats in (L-O-D), vide infra.

Spin–Lattice Relaxation. The analysis of the coupling constants of three Pro-containing cyclic tripeptides presented above shows a picture of proline rings existing in rapid dynamic conformational equilibrium or, in other cases, displaying large-amplitude torsional oscillations. These conformational degrees of freedom (ring flip and oscillation) can be monitored qualitatively by means of the spin–lattice relaxation times, T, of the ring-carbon atoms, provided the dipolar relaxation mechanism predominates. The measured nuclear Overhauser effects (NOE) ensure that this condition is met.[24,27] Thus the nT_1 values (n is the number of hydrogen atoms directly bonded to the carbon atom measured) are correlated with the intramolecular mobility of the proline rings in solution via the changes in direction of the C–H vectors. These changes, e.g., from pseudoaxial to pseudoequatorial, are correlated with the movement of the C atoms perpendicular to the mean plane of the ring.

(33) Bats, J. W.; Fuess, H., to be published.

Table V. ^{13}C NMR Spin-Lattice Relaxation Times (nT_1) in *cyclo*(L-Pro^1-L-Pro^2-D-Pro^3)[a] and *cyclo*(L-Pro^1-BzlGly-D-Pro^3)[b]

compd	C^α	C^β	C^γ	C^δ	X_S[c]
(L L-D)					
L^1	0.85	1.40	1.70	1.26	0.21
L^2	1.04	1.56	1.76	1.24	0.37
D^3	0.94	0.96	1.20	1.14	*d*
(L-0-D)					
L^1	0.83	1.39	1.49	1.15	0.33
D^3	0.84	1.01	1.10	1.30	*d*

[a] Data taken from ref 36. [b] Data taken from ref 27. [c] Mole fraction of *S* conformer calculated from NMR coupling constants (see Table II). [d] Oscillating single state.

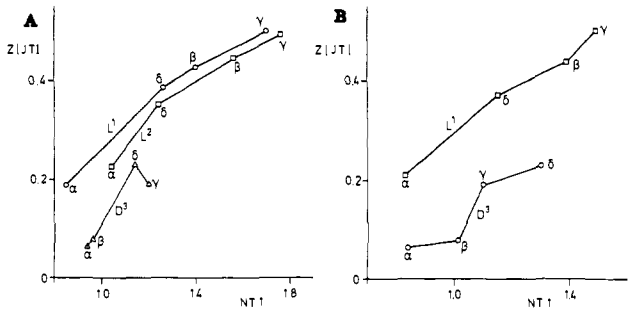

Figure 4. Correlation of total atomic displacements Z_j^t (Å) from force-field calculations and ^{13}C NMR spin-lattice relaxation times nT_1 (s) for L-Pro^2 in *cyclo*(L-Pro^1-L-Pro^2-D-Pro^3) (A) and in *cyclo*(L-Pro^1-BzlGly-D-Pro^3) (B).

For an inversion barrier of less than about 5 kcal/mol, the transition between *N* and *S* states is very fast at ambient temperature (less than 1 ns), but still much slower than torsional oscillations. In the case of a roughly 50/50 ${}_\beta^\gamma T \rightleftarrows {}_\gamma E$ equilibrium (cf., L-Pro^2 in (L-L-D), Table II) one predicts C^α to have the smallest movement perpendicular to the mean plane of the ring, and increasing movements of C^δ, C^β, and C^γ in this order. These movements are approximated by eq 9, introduced by Kilpatrick

$$Z_j = (2/5)^{1/2} q \cos(\psi + 4\pi j/5) \qquad j = 0 \ldots 4 \qquad (9)$$

et al.,[34] where $\psi = P - 90°$; Z_j is the distance of the atom *j* to the mean plane; *q* is the maximum displacement from this plane. Translated into relaxation times, one expects increasing nT_1 values in the order: C^α, C^δ, C^β, C^γ. This expectation is borne out well. Figure 4 shows interesting correlations between the total atomic displacements, Z_j^t,[35] for the ${}_\beta^\gamma T \rightleftarrows {}_\gamma E$ inversion and the experimental nT_1 values for (L-L-D)[36] and (L-0-D).[27] However, as the conformational equilibrium shifts away from a 50/50 mixture toward a more biased situation, these approximations will probably tend to fail. Nevertheless, as the equilibrium shifts toward one side or another the carbon atoms remain for a longer period of time in the preferred form, which leads to reduced nT_1 values. Therefore, it is predicted that smaller nT_1 values correspond to a more biased *N*/*S* equilibrium. Indeed, the trend found for the L-Pro^1 and L-Pro^2 residues in (L-L-D) agrees roughly with the *N*/*S* ratios calculated from the NMR coupling constants (Table V). The D-Pro^3 residue appears to remain in a single oscillating conformation (vide supra) and, accordingly, the nT_1's are even further decreased (Figure 4). A similar correlation has been found for the thermal *U* parameters of the X-ray structures and nT_1 values.[24,27,36]

Barfield Transmission Effect. On the basis of the generalized Karplus equation one predicts that, regardless of the model used, pairs of cis coupling obey the following approximate equalities over the entire pseudorotation itinerary: $J_{24'} \simeq J_{34}$ and $J_{46} \simeq J_{4'5}$. Indeed, the calculated differences between these couplings do not exceed 0.4 Hz. However, a close examination of the experimental results reveal that the true difference can be larger than 1.0 Hz (Table III).

Two possible explanations for this discrepancy are envisaged: (i) geometry perturbations of the proline ring in cyclic tripeptides compared to prolines in open-chain peptides, (ii) the presence of an extra coupling pathway which specifically influences certain cis couplings. The first explanation seems unlikely to be correct because an analysis of the available X-ray structures of cyclic tripeptides containing proline[23,29,33,37] indicates that the torsion angle correlations, embodied in eq 2, are also valid for cyclic tripeptides. The second explanation appears more attractive. It is known that, through the operation of the "Barfield transmission effect",[38] the magnitude of the vicinal cis couplings can be strongly influenced. For example, in the highly puckered envelope geometry of norbornanes the through-space interaction between the carbon-hydrogen orbitals of the C_2–C_3 fragment with the orbitals of the C_7 methylene bridge causes a relative decrease of the endo–endo (cis) coupling constant with respect to the exo–exo (cis) coupling. In a general five-membered ring, one expects that the Barfield effect would tend to relatively and significantly reduce the cis couplings between pairs of protons located trans with respect to the carbon or heteroatom that resides at, or near to, the "flap" of the envelope. Indeed, calculations employing the finite perturbation theory (FPT) have demonstrated that the Barfield effect operates in cyclopentane as well as in oxolane.[39] Similar IND-O-FPT calculations, carried out by the Leiden group,[40] show that the same effect is operational in prolines. For example, the calculations predict that for an αE ($P \simeq 126°$) conformation, $J_{4'5} < J_{46}$ and $J_{34} < J_{24'}$. The calculated values are $J_{4'5} = 11.7$ Hz; $J_{46} = 12.8$ Hz; $J_{34} = 11.2$ Hz; $J_{24'}$, 11.9 Hz. Although these numbers are slightly too high, it is gratifying to note that the FPT calculations predict trends that are quantitatively in line with the experimental results for (L_3) and for both D-Pro^3 residues, Table III, which proline rings have a strong preference for *S*-type geometry. Thus far, no FPT calculations for *N*-type geometries are available, but on grounds of symmetry considerations it is expected that the trend will be reversed. This expectation is borne out by the experimental findings: in the L-Pro^1 residue of the tripeptide (L-L-D) one has $J_{4'5} > J_{46}$ and $J_{34} > J_{24'}$, Table III. In the present state of our knowledge it is not deemed practically possible to incorporate a correction for the Barfield effect in the program PSEUROT. However, errors in the cis couplings will mainly influence the magnitude of the calculated amplitude of pucker χ_m, whereas the more important phase angle parameter as well as the calculated mole fraction largely depend on the trans couplings and the latter remain unaffected by this through-space effect. Obviously, the rms value would decrease significantly in the absence of alternative coupling pathways.

Conformations of the Peptide Backbone. The formal conformational analogy between cyclic tripeptides and cyclohexane has been pointed out before by us.[30] Replacement of the peptide bond by a dummy atom leads from the so-called crown conformation of the cyclotripeptide to the rigid chair form of cyclohexane and from a boat or twist-boat peptide to a boat or twist-boat cyclohexane. It is therefore easy to see that in principle not more than two inverting crown forms can exist although only one is often preferred because of restrictions imposed by the chirality of the amino acids and the bulk of the side chains. A total of six boat conformations are encountered during pseudorotation, interspersed with six twist-boat forms. In principle one can think of a pseudorotation phase angle formalism according to which the six boat

(34) Kilpatrick, J. E.; Pitzer, K. S.; Spitzer, R. *J. Am. Chem. Soc.* **1947**, *69*, 2483–2488.
(35) The total atomic displacement $Z_j t$ of atom *J* during the conformational *N*/*S* inversion is defined as $|Z_j N - Z_j S|$.
(36) Kessler, H.; Friedrich, A.; Krack, G.; Hull, W. E. *Pept. Proc. Am. Pept. Symp. 7th*, **1981**, 335–338.
(37) Kartha, G.; Ambady, G. K. *Acta Crystallogr., Sect. B* **1975**, *B31*, 2035–2039.
(38) Marshall, J. L.; Walter, S. R.; Barfield, M.; Marchand, A. P.; Marchand, N. W.; Segre, A. L. *Tetrahedron* **1976**, *32*, 537–542.
(39) Jaworski, A.; Ekiel, I.; Shugar, D. *J. Am. Chem. Soc.* **1978**, *100*, 4357–4361.
(40) De Leeuw, F. A. A. M.; Van Beuzekom, A. A.; Altona, C. *J. Compt. Chem.*, in press.

Table VI. Backbone Torsion Angles[a] in *cyclo*(L-Pro$_3$), *cyclo*(L-Pro$_2$-D-Pro), and *cyclo*(L-Pro-BzlGly-D-Pro) from the Averaged X-ray Structure and from Force-Field (FF) Minimizations

compd		ω_1	ϕ_1	ψ_1	ω_2	ϕ_2	ψ_2	ω_3	ϕ_3	ψ_3
(L_3)	X-ray[b]	2	−98	93	2	−98	93	2	−98	93
	FF	−9	−88	100	−9	−88	100	−9	−88	100
(L-L-D)	X-ray[c]	−15	−46	108	7	−51	−21	−3	106	−52
	FF *NNS*	−6	−54	108	5	−46	−30	13	99	−62
	SNS	0	−62	108	8	−45	−32	11	100	−63
	NSS	−3	−53	107	10	−59	−20	12	98	−66
	SSS	2	−61	107	12	−57	−22	10	99	−67
(L-0-D)	X-ray[d]	−7	−47	111	2	−66	1	−4	100	−62
	FF *TB*-1-*NS*[e]	−4	−53	107	9	−59	−17	10	98	−65
	TB-1-*SS*	1	−61	108	12	−56	−22	9	99	−65
	TB-2-*SS*	−10	−99	65	2	57	−108	−11	57	21
	TB-2-*SN*	−11	−101	61	4	59	−109	−7	45	31

[a] See Figure 5. [b] Reference 29. [c] Reference 23. [d] Reference 33. [e] See text for nomenclature.

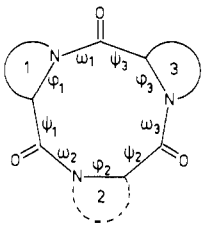

Figure 5. Numbering of the backbone angles in cyclic tripeptides.

forms of the cyclotripeptide occur at 0°, 60°, 120° ... and the intermediate twist-boats at 30°, 90°, 150°, ...[41] The quantitative application of such a formalism requires consensus as to the definition of the starting point (P 0°) and for the time being it suffices to use the concept of pseudorotation in a more qualitative fashion. It is important to note that the presence of prolyl residues severely restricts the available conformational range along the boat-twist boat itinerary.[30] This restriction arises, aside from steric interferences, from the fact that the chirality of the prolyl residue fixes the sign of backbone angle ϕ(C′–N–C$^\alpha$–C′). In the L-Pro series this angle has a value of about −40° in cyclic dipeptides and ranges from −46° to −110° in cyclotripeptides[7] but is always negative. In the D-Pro series angle ϕ is necessarily positive. Free pseudorotation implies sign inversions at 180° intervals of the phase angle, and this is evidently impossible when one or more proline residues are present. See Figure 5 for the ϕ, ψ, ω rotation.

The magnitude adopted by ϕ_i (i = 1, 2, 3) in the nine-membered ring influences the conformational freedom of the attached Pro^i residue via χ_5. A survey of X-ray structures has shown that in cyclic peptides (except dipeptides) of the L series the magnitude of the difference $\chi_5 - \phi$ invariably occurs in the range 60–80°, average 70° ± 6°.[7] This means that for $|\phi| < 60°$, χ_5 must be >+10° and this condition can be met either by a normal N conformation or by a distorted S-type form ($P \gg 198°$). For $|\phi| > 80°$, torsion angle χ_5 must be <−10° and the L-Pro ring is forced to adopt either an S-type geometry or a distorted N form. In the intermediate range of ϕ the prolyl ring has access to both normal N and S conformations. For the D series one expects a correlation $-\chi_5 + \phi \sim 70°$ and a corresponding rule will hold.

Let us now examine the results of the coupling constant analysis in the light of the known X-ray structures and with the aid of molecular mechanics calculations. These calculations were carried out by means of program UTAH-5[42] with the use of the force-field parametrization of DeTar and Luthra.[6] One additional parameter was required in order to reproduce the small deviation of the amide nitrogen from planarity. By trial and error it was found that a force constant of 6 kcal/mol for out-of-plane bending gave satisfactory results and this value was employed in the present work.

The crown conformation adopted by (L_3) in the solid state requires ϕ to lie in the range 94.8°–106°, mean 97.6°. As a consequence, the L-Pro residues are forced to adopt an S-type

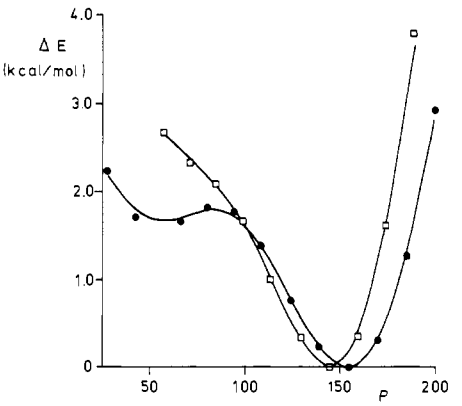

Figure 6. Calculated conformational energy upon pseudorotation of L-Pro^1 in *cyclo*(L-Pro^1-L-Pro^2-L-Pro^3) (closed circles) and of D-Pro^3 in *cyclo*[L-Pro^1-Gly-D-Pro^3) (open squares, *TB*-1-*NS* conformer, see text) at constant puckering of 35°.

conformation corresponding to a $^{\beta}_{\alpha}T$ geometry. The conformational details of the crown backbone as detected by X-ray crytallography are well reproduced by the molecular mechanics method, Table VI. Moreover, the calculations help us to understand the oscillating phase angle model postulated from the coupling constant analysis.

The UTAH program allows the fixation of one or more torsion angles to a preset value. This technique was employed to drive the phase angle of pseudorotation of one of the proline rings, say L-Pro^1, in discrete steps over a large range at a constant puckering amplitude of 35°. Except for the one or two fixed torsion angles all the remaining internal degrees of freedom were allowed to relax and the geometry and conformational energy was calculated at 15° intervals of P_1. Details of the geometry changes will be reported elsewhere;[40] here it suffices to say that changes in P_1 are reflected foremost by changes in ϕ_1 and ω_1, to a lesser extent by changes in ψ_1, ω_2, and ω_3 and hardly by changes in the remaining backbone angles. The L-Pro^2 and L-Pro^3 residues are not significantly affected when L-Pro is forced to pseudorotate from P 25° to 200°. This means that each Pro residue oscillates independently from the two other ones. A plot of the calculated conformational energy vs. P is shown in Figure 6. The potential energy profile displays a major minimum at P 155°, appears rather shallow (width about 60° along the P axis at 1 kcal/mol above the global minimum) and significantly skewed toward the lower P values. Interestingly, a secondary minimum was found at about $P \sim 70°$. Full relaxation of the calculation yielded an N-type conformer characterized by P_N 75°, χ_N 32°, and an energy of 1.6 kcal/mol above the global minimum. The calculations cannot be taken to prove the physical existence of this minor N conformation in (L_3), but it should be noted that the hydroxyprolyl residue in crystalline[37] *cyclo*(L-Pro$_2$-L-Hyp) adopts a closely similar geometry P_N 77°, χ_N 35°, with the cyclic backbone in a crown conformation similar to that of (L_3). This suggests that the force-field calculations may well be correct. The preference of

(41) Buys, H. R.; Geise, H. J. *Tetrahedron Lett.* **1968**, *54*, 5619–5624.
(42) Faber, D. H.; Altona, C. *Comput. Chem.* **1977**, *1*, 203–213.

L-Hyp for the *N* conformation is seen as a manifestation of the stabilizing gauche O–C$^{\gamma}$–C$^{\delta}$–N interaction.[7] The force-field prediction of a minimum-energy form at *P* 75° prompted us to carry out the PSEUROT calculations also for this value of the phase angle, Table II.

Three chiral amino acids in the cyclic tripeptide ring, one of which has opposite chirality with respect to the other two, serve to limit the available conformational freedom to a single twist-boat form. This is predicted[30] to be the case for (L^1-L^2-D^3). However, although the peptide backbone ring may be considered "rigid", the NMR coupling constant and nT_1 data clearly show that the L-prolyl residues still have some conformational freedom left, vide supra. Table II reveals that the major conformational preference for L-Pro^1 and L-Pro^2 is *N*, that for D-Pro^3 is *S*, but the former residues can flip into *S*-type conformers (populations of 21% and 37%, respectively). The NMR data do not tell us whether or not these interconversions occur in a mutually independent fashion. In order to supply an answer to this question, a series of force-field calculations was carried out. Four stable minima were found, denoted *NNS*, *SNS*, *NSS*, and *SSS*, with corresponding calculated conformational energies of 0, 0.42, 1.36, and 1.93 kcal/mol, respectively. All attempts to calculate a stable *N* conformer for the D-Pro residue failed. It is seen that the force-field calculations predict that L-Pro^1 should show greater relative proclivity toward flipping into the *S* state than would L-Pro^2, contrary to experiment. The reasons for this discrepancy are unclear, but for the time being we tend to place more trust in the calculated geometries than in the corresponding conformational energies.

In further calculations the L-Pro^1 ring of the *NNS* species was driven from *P* 340° to 40° in steps of 10° in phase angle (χ_N 35°) in order to explore the shape of the potential energy well. It turned out (not shown) that the well corresponded nearly perfectly to a harmonic oscillator. Furthermore, the local conformations adopted by each of the individual L^1, L^2, and D^3 rings appeared to be virtually independent of the actual conformation adopted by the other two. As was the case with the crown form of (L$_3$), the twist-boat of (L-L-D) does not allow conformational transmission effects to operate from one prolyl residue to another. The *N*/*S* interconversion of L^1 and L^2 results only in relatively small changes of the backbone angles ϕ, ψ, and ω, localized about the L-Pro residue involved, Table VI. These findings imply that, although four conformations altogether partake in the equilibrium, a two-scale model remains operationally correct for the description of L^1 and L^2.

The energy well of the D^3 residue in (L-L-D) was not investigated in detail, but there is every reason to assume that its general properties are very similar to those calculated for the D-Pro^3 residue in (L-0-D), described below.

Let us finally examine the results obtained for (L-0-D). Cyclic tripeptides of this type, with the Pro residues differing in chirality, are predicted[30] to have access to two different twist-boat conformations, interconverting via a true boat form. In the solid state only one of these predicted forms is found;[33] this conformation is characterized by ϕ_1 −46° and ϕ_3 +106°, Table VI. The prolyl residues conform to the conformational preferences already noted in the case of (L-L-D) and L-Pro^1 takes up an *N*-type geometry whereas D-Pro^3 assumes the familiar *S* form. It was shown by the ^{13}C data before[25] and proven in this paper (see above) that the geometry of the preferred conformations of these prolyl residues in solution, as deduced from the NMR spin–spin coupling constants, appears to agree well with that found in the crystal (Table II). Therefore, it is concluded that the twist-boat backbone conformer detected in the crystal (*TB*-1) corresponds to the (major) species present in solution.[43] The existence of a minor amount of the second twist-boat (*TB*-2) conformer cannot be rigidly excluded, however. The *TB*-2 backbone has the positions of the peptide residues interchanged to read: (0^1-D^2-L^3). In other words, one expects that in *TB*-2 the D-Pro residue has the same preference for *N*-type form as is displayed by L-Pro^2 in (L^1-L^2-D^3). By the same token, the L-Pro residue of *TB*-2 should share the properties of D-Pro^3 in (L-L-D), i.e., adopt an (oscillating) *S*-type ring conformation. The coupling constant analyses (Table II) show that D-Pro^3 in (L^1-0^2-D^3) appears to have a higher population of *N* and L-Pro^1 a higher population of *S* form than expected on the basis of the results obtained for (L-L-D). These findings can be rationalized by the assumption of a small amount (<20%) of *TB*-2 in equilibrium with *TB*-1. If this were the case, we have a four-state equilibrium for each prolyl residue in (L-0-D) and the geometries derived from the two-state analysis represent a weighted average.

Force-field calculations[44] again serve to clarify the situation. In order to avoid confusion because of nomenclature problems, we propose to adhere to the following notation: in conformational sequences as *NS*, *SS*, and *SN* the first letter denotes the conformation of the L-Pro residue, the second that of D-Pro, irrespective of their position (1, 2, or 3) on the cyclic backbone. The conformation present in the crystal structure then corresponds to *TB*-1-*NS*.

As expected from our force-field study on (L$_3$) and (L-L-D), vide supra, the prolyl residues are predicted to enjoy limited conformational freedom when the adjoining ϕ angle adopts a value in the 60° range (L-Pro in *TB*-1, D-Pro in *TB*-2). The calculations yielded four stable minima; *TB*-1-*NS*, *TB*-1-*SS*, *TB*-2-*SN*, and *TB*-2*SS*. The corresponding backbone angles are shown in Table VI. The calculated relative energies (not shown) would predict *TB*-2-*SN* to be more stable by about 1.3 kcal/mol with respect to *TB*-1-*NS*, in contradiction to experiment, but cf. ref 43.

In order to detect the suspected existence of a skewed potential and of a secondary minimum for those Pro residues that are forced to adopt an *S*-type geometry by the attached high ϕ angle (90–110°), these conformations were driven over a large range of *P* as described above in the case of (*L*$_3$). Both D-Pro in *TB*-1-*NS* and L-Pro in *TB*-2-*SN* were studied. The results were virtually identical: the potential energy well appears skewed and we find no indications for a secondary minimum, Figure 6.

The two twist-boat conformations are related by restricted pseudorotation via true boat which is characterized by $\phi_2 \sim \psi_3 \sim 0°$. The next logical step was the computer exploration of this saddle point in order to gain an impression of the transition energy involved. By driving ϕ_2 and ψ_3 simultaneously in steps of about 10° and allowing complete relaxation of the geometry after each step (except for the angles driven), a saddle point was found with ϕ_2 7°, ψ_3 −17° and an energy of only 3.0 kcal/mol above that calculated for the start conformation *TB*-2-*SS*. The same saddle point was reached starting from *TB*-1-*SS*, which has a calculated ground-state conformational energy 0.3 kcal/mol below *TB*-2-*SS* and 0.2 kcal/mol above *TB*-1-*NS*. Even allowing for the fact that the calculated conformational energies apparently cannot be trusted too much, the conclusion must be that the energy barrier is quite low and the rate of interconversion between the two *TB* conformers correspondingly extremely fast on the NMR time scale.

Conclusion

The symmetrical crown conformation of (L$_3$) has ϕ angles near −100°, as a consequence the L-Pro residues are forced to adopt a conformation in the *S*-region (near ${}^{\beta}_{\alpha}T$). Some pseudorotational freedom remains available to these residues, however. Large-amplitude oscillations of the phase angle are possible inside a skewed potential energy well. A secondary minimum is perhaps located near ${}^{N}_{\delta}T$, but this minimum also can be viewed as part of the conformational continuum about the global minimum. The oscillations of the three residues are independent of each other according to the force-field calculations.

The cyclic tripeptide (L^1-L^2-D^3) assumes a single twist-boat conformation. The values of ϕ_1 and ϕ_2 (about −50°) are such that

(43) This conclusion hinges on the correct assignment of one particular group of ^{1}H and ^{13}C resonances to L-Pro^1 and of the other group to D-Pro^3. However, the second possible twist-boat form (*TB*-2) has the positions of the peptide residues interchanged: (0^1-D^2-L^3), and this sequence does not fit the established ^{1}H and ^{13}C chemical shift patterns.[25] The vicinal coupling constants do not allow for a verdict one way or another.

(44) The benzyl group was replaced by methyl in order to reduce computer time.

the L-Pro[1] and L-Pro[2] residues enjoy true conformational freedom; these rings can flip from the major *N*-type conformation (in the ${}^{\beta}T-{}^{\gamma}E$ region) into a minor *S* form (probably near to ${}_{\gamma}E$). This freedom is more pronounced in L-Pro[2] than it is in L-Pro[1]. Moreover, the flipping occurs in an independent fashion and not concerted. The D-Pro[3] residue appears to carry out large-amplitude oscillations inside a skewed well.

Matters appear more complicated in the case of (L[1]-0[2]-D[3]). The proposed existence[30] of two different twist-boat conformations of the nine-cycle is corroborated by the force-field minimizations. In each of the twist boats the two prolyl residues are predicted to enjoy some measure of conformational freedom, one of the flipping type, the other of the oscillating type. The coupling constant analysis leads to the conclusion that the two twist-boat froms cannot be present in nearly equal amounts but that one of them strongly predominates in solution. The predominant twist-boat resembles that found in the crystal.

Acknowledgment. We thank A. A. van Beuzekom for his assistance in the force-field calculations.

Registry No. *cyclo*(L-Pro$_3$), 2277-82-9; *cyclo*(L-Pro$_2$-L-Pro), 70493-40-2; *cyclo*(L-Pro-BzlGly-D-Pro), 85026-16-0.

Electrochemical Characterization of p-Type Semiconducting Tungsten Disulfide Photocathodes: Efficient Photoreduction Processes at Semiconductor/Liquid Electrolyte Interfaces

Joseph A. Baglio,*[1] Gary S. Calabrese,[2] D. Jed Harrison,[2] Emil Kamieniecki,[1] Antonio J. Ricco,[2] Mark S. Wrighton,*[2] and Glenn D. Zoski[1]

Contribution from the Department of Chemistry, Massachusetts Institute of Technology, Cambridge, Massachusetts 02139, and Advance Technology Laboratory, GTE Laboratories, Inc., Waltham, Massachusetts 02254. *Received August 23, 1982*

Abstract: Single-crystal p-type WS_2 ($E_g \approx 1.3$ eV) has been synthesized and characterized as an electrode material in CH_3CN/0.1 M $[n\text{-}Bu_4N]ClO_4$ and in aqueous electrolytes containing a variety of one-electron redox reagents having different $E_{1/2}$ values. In either CH_3CN or H_2O solvent the flat-band potential, E_{FB}, is measured to be $\sim$+0.95 V vs. SCE. In aqueous I_3^-/I^- the E_{FB} is shifted more negative by at least 0.3 V as is found for n-type WS_2 photoanodes. Capacitance measurements of the WS_2/electrolyte interface to determine E_{FB} accord well with electrochemical measurements. For $E_{1/2}$ more negative than E_{FB} the p-type WS_2 behaves as a photocathode giving an open-circuit photovoltage, E_V(oc), up to $\sim$0.8 V depending on $E_{1/2}$. For $E_{1/2}$ between +1.3 and −0.1 V vs. SCE, E_V(oc) varies as expected: for $E_{1/2}$ more positive than E_{FB} the p-type WS_2 behaves as a metallic electrode while for $E_{1/2}$ more negative than E_{FB} we find $E_V(oc) \approx |E_{1/2} - E_{FB}|$. It appears that for negative redox couples carrier inversion results at the p-WS_2 surface, but for $E_{1/2}$ more negative than −0.1 V vs. SCE E_V(oc) declines, a result associated with junction breakdown at sufficiently negative potentials. p-Type WS_2-based photoelectrochemical cells can be used to effect the sustained conversion of visible light (632.8 nm) to electricity in H_2O or CH_3CN with efficiencies of up to $\sim$7%. In H_2O the photochemical reduction to H_2 can be effected by illumination of p-type WS_2 modified by depositing $\sim 10^{-7}$ mol/cm^2 of Pd(0) or Pt(0) onto the surface as an H_2 evolution catalyst. Efficiency for H_2 evolution from 6 M H_2SO_4 is typically 6-7% for 632.8 nm (50 mW/cm^2) intensity.

There has been much interest in n-type semiconducting metal dichalcogenide, MY_2, electrodes for use in photoelectrochemical devices for conversion of light to electricity or chemical energy.[3-10] Efficient optical energy conversion has been realized with n-type MY_2 photoanodes, including a report of >10% efficiency for the

(1) GTE Laboatories, Inc.
(2) Massachusetts Institute of Technology.
(3) (a) Tributsch, H.; Bennett, J. C. *J. Electroanal. Chem.* **1977**, *81*, 97. (b) Tributsch, H. *Z. Naturforsch. A*, **1977**, *32A*, 972; *J. Electrochem. Soc.* **1978**, *125*, 1086; **1981**, *128*, 1261; *Ber. Bunsenges. Phys. Chem.*, **1977**, *81*, 361; **1978**, *82*, 169; *Sol. Energy Mater.* **1979**, *1*, 257; *Discuss. Faraday Soc.* **1980**, *70*, 189. (c) Gobrecht, J.; Tributsch, H.; Gerischer, H. *J. Electrochem. Soc.* **1978**, *125*, 2085; *Ber. Bunsenges. Phys. Chem.* **1978**, *82*, 1331. (d) Ahmed, S. M.; Gerischer, H. *Electrochim. Acta* **1979**, *24*, 705. (e) Kautek, W.; Gerischer, H.; Tributsch, H. *Ber. Bunsenges. Phys. Chem.* **1979**, *83*, 1000; *J. Electrochem. Soc.* **1980**, *127*, 2471. (f) Tributsch, H.; Gerischer, H.; Clemen, C.; Bucher, E. *Ibid.* **1979**, *83*, 655. (g) Kautek, W.; Gerischer, H. *Ber. Bunsenges. Phys. Chem.* **1980**, *84*, 645. (h) Kautek, W.; Gobrecht, J.; Gerischer, H. *Ibid.* **1980**, *84*, 1034. (i) Jaeger, C. D.; Gerischer, H.; Kautek, W. *Ibid.* **1982**, *86*, 20. (j) Clemen, C.; Saldana, X. I.; Muny, P.; Bucher, E. *Phys. Status Solidi A* **1978**, *49*, 437.
(4) (a) Lewerenz, H. J.; Heller, A.; DiSalvo, F. J. *J. Am. Chem. Soc.* **1980**, *102*, 1877. (b) Menezes, S.; DiSalvo, F. J.; Miller, B. *J. Electrochem. Soc.* **1980**, *127*, 1751. (c) Menezes, S.; Schneemeyer, L. F.; Lewerenz, H. J. *Appl. Phys. Lett.* **1981**, *38*, 949. (d) Lewerenz, H. J.; Ferris, S. D.; Doherty, C. J.; Leamy, H. J. *J. Electrochem. Soc.* **1982**, *129*, 418.
(5) (a) Fan, F.-R. F.; White, H. S.; Wheeler, B.; Bard, A. J. *J. Electrochem. Soc.* **1980**, *127*, 518. (b) Fan, F.-R. F.; White, H. S.; Wheeler, B. L.; Bard, A. J. *J. Am. Chem. Soc.* **1980**, *102*, 5142. (c) Abruna, H. D.; Bard, A. J. *J. Electrochem. Soc.* **1982**, *129*, 673. (d) White, H. S.; Abruna, H. D.; Bard, A. J. *Ibid.* **1982**, *129*, 265. (e) White, H. S.; Fan, F.-R. F.; Bard, A. J. *Ibid.* **1981**, *128*, 1045. (f) Nagasubrmanian, G.; Bard, A. J. *Ibid.* **1981**, *128*, 1055. (g) Frank, S. N.; Bard, A. J. *J. Am. Chem. Soc.* **1975**, *97*, 7427. (h) Laser, D.; Bard, A. J. *J. Am. Chem. Soc.* **1976**, *80*, 459.
(6) (a) Schneemeyer, L. F.; Wrighton, M. S. *J. Am. Chem. Soc.* **1979**, *101*, 6496; **1980**, *102*, 6964. (b) Schneemeyer, L. F.; Wrighton, M. S.; Stacy, A.; Sienko, m. J. *Appl. Phys. Lett.* **1980**, *36*, 701. (c) Kubiak, C. P.; Schneemeyer, L. F.; Wrighton, M. S. *J. Am. Chem. Soc.* **1980**, *102*, 6898. (d) Calabrese, G. S.; Wrighton, M. S. *Ibid.* **1981**, *103*, 6273.
(7) (a) Kline, G.; Kam, K.; Canfield, D.; Parkinson, B. A. *Sol. Energy Mater.* **1981**, *3*, 301. (b) Canfield, D.; Parkinson, B. A. *J. Am. Chem. Soc.* **1981**, *103*, 1249. (c) Furtak, T. E.; Canfield, D.; Parkinson, B. A. *J. Appl. Phys.* **1980**, *51*, 8018. (d) Parkinson, B. A.; Furtak, T. E.; Canfield D.; Kam, K.; Kline, G. *Discuss. Faraday Soc.* **1980**, *70*, 233.
(8) Baglio, J. A.; Calabrese, G. S.; Kamieniecki, E.; Kershaw, R.; Kubiak, C. P.; Ricco, A. J.; Wold, A.; Wrighton, M. S.; Zoski, G. D. *J. Electrochem. Soc.* **1982**, *129*, 1461.

0002-7863/83/1505-2246$01.50/0